

# PERIODIC MULTI-MODE BATCH DRYING OF HEAT-SENSITIVE MATERIALS- ENGINEERING APPLICATIONS OF THE DIFFUSION EQUATION

Md. Raisul Islam and A.S. Mujumdar

## 1. INTRODUCTION

The main objective of this chapter is to provide a summary of the results and useful conclusions one can draw by solving the liquid diffusion equation under a wide assortment of boundary conditions. Aside from calculation of drying times for batch drying one can readily examine the potential of applying multiple sources of heat continuously or intermittently without exceeding the thermal damage temperature of the product. It can answer such questions of engineering importance as: what is the best range over which a heat pump may be applied or over what range of moisture contents should one apply microwave heating for cost-effective results. We can also simulate solar drying wherein the solar insulation level is necessarily time-dependent. If we insert a model for color degradation kinetics or degradation of nutritional value with temperature, we can also predict the ultimate dried product quality as well. Since drying kinetics of heat sensitive products are necessarily low, the drying times for a single experiment can exceed 4-5 hours. If one looks at the multitude of parameters that are present even in the relatively simple one-dimensional problem, it is readily seen that a purely experimental approach to seeking an optimal design of a dryer is nearly impossible. It is essential to resort to some simple mathematical models to reduce the need for experimentation to a minimum. We need certain properties and transport coefficients to solve the model equations. Once we have them, we can evaluate the effects of various parameters and try to obtain an optimal engineering design with only a few validation experiments. This, indeed, is the goal of this study.

## 2. THE MATHEMATICAL MODEL

Despite its remarkable simplicity and empirical origin, the falling rate period for many materials that must be dried at moderate temperatures so that no phase change occurs within the material itself but only at the evaporating surface, can be well described by the classical diffusion model. A diffusive process is one for which the local flux is proportional to the local gradient serving as the driving force e.g. concentration difference for mass transfer. In drying this coefficient of proportionality is often a strong function of the moisture content as well as temperature. Indeed, we have shown that it must also depend on porosity or shrinkage of the material. Here we will not examine the complicating factors, but only focus on an application which requires solution to the one dimensional diffusion equation in Cartesian system subject to a variety of boundary conditions. We consider a non-isothermal case so that the diffusion equation must be solved concurrently with the energy equation. The heat and mass transfer during the drying process is shown schematically in Figure 1. Since the diffusivity of moisture and heat are both dependent on temperature and moisture content, the equations are fully coupled and nonlinear.

We consider the hygro-thermal properties using a slab of potato as model material subjected to drying on one side by convection alone, by convection and conduction from the bottom face, convection and radiation from the evaporating surface as well as convection and microwaves. The effect of including the physically realistic shrinkage but with moisture (liquid phase) diffusivity un-corrected for shrinkage is also included.

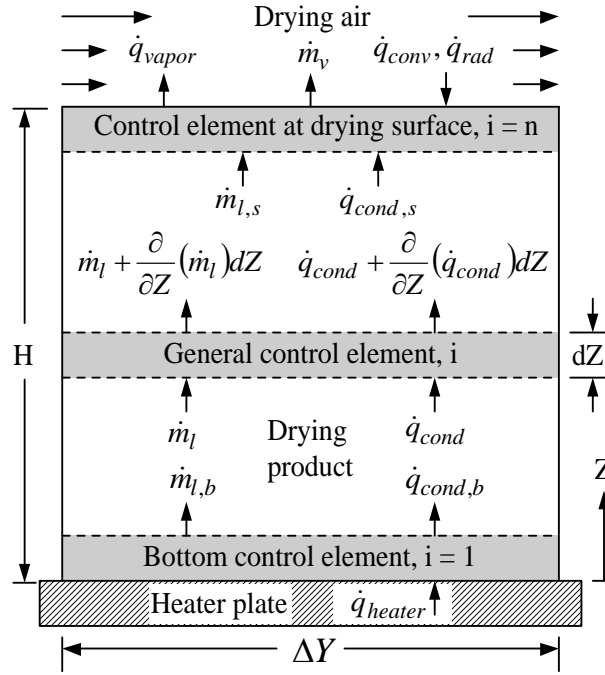


**Figure 1.** Schematic of the control volume for the physical model

## 2.1 Assumptions

The following assumptions are made in developing the present physical model applicable to one-sided drying of a thin slab like material:

1. The drying product is compact, homogeneous and without voids with trapped air.
2. The temperature and moisture content are initially uniform inside the product.
3. Mass diffusivity, thermal conductivity and density of product are known functions of moisture content and temperature of the product.
4. The product shrinks ideally during drying, i.e. the volume occupied by the dry matter and water decreases by an amount equal to that of evaporated water. This assumption can be relaxed if real shrinkage data are available.
5. Heat transfer by conduction and liquid moisture transfer by diffusion govern the drying rate. No deformation other than shrinkage in the thickness direction occurs as a result of drying.
6. Moisture transfer inside the product in the vapor phase is negligible compared to that in the liquid phase (low temperature drying). No phase change occurs within the drying material i.e. evaporation occurs only at the evaporating surface.

Despite the large number of assumptions, the model is applicable to a large number of products dried in practice.

## 2.2 Governing Equations

The energy conservation equation for the general control volume considering heat is transferred only by conduction process in the Z-direction can be expressed as

$$\rho_p C_p \frac{\partial T_p}{\partial t} = \frac{\partial}{\partial Z} \left( k_p \frac{\partial T_p}{\partial Z} \right) + Q_{mw}(X_m, Z, t) \quad (1)$$

where  $Q_{mw}$  is the microwave source term which is a function of the dry basis moisture content,  $X_m$ , at different depth of the product. (See nomenclature for meaning of symbols.)

Due to the dissipation of microwave power, the generated heat at depth (H-Z) from the drying surface can be determined as [Sanga et al., 2002]

$$Q_{mw}(X_m, Z, t) = 2Q_{mw,o}\beta \exp[-2\beta(H - Z)] \quad (2)$$

where  $Q_{mw,o}$  is the incident microwave flux at the drying surface of the product and  $\beta$  is the attenuation constant which can be expressed in terms on dielectric properties of material as

$$\beta = \frac{2\pi}{\lambda_{mw,v}} \sqrt{\frac{\varepsilon' \left[ \left\{ 1 + \left( \frac{\varepsilon''}{\varepsilon'} \right)^2 \right\}^{1/2} - 1 \right]}{2}} \quad (3)$$

where  $\lambda_{mw,v}$  is the wavelength in vacuum.  $\varepsilon'$  and  $\varepsilon''$  are the dielectric constant and the dielectric loss factor respectively which depend on product temperature, moisture content and product density.

The thermal conductivity for transferring heat from control volume i to i+1 can be expressed as

$$k_{p(i \text{ to } i+1)} = \frac{\Delta Z_i + \Delta Z_{i+1}}{\frac{\Delta Z_i}{k_{p(i)}} + \frac{\Delta Z_{i+1}}{k_{p(i+1)}}} \quad (4)$$

The species transport equation for liquid moisture with diffusion only in the Z-direction can be written as

$$\frac{\partial \rho_m}{\partial t} = \frac{\partial}{\partial Z} \left( \rho_p D_{AB} \frac{\partial \rho_m}{\partial Z} \right) \quad (5)$$

Similarly the diffusivity for the migration of moisture from control volume i to i+1 gives

$$\rho_p D_{AB} \Big|_{i \text{ to } i+1} = \frac{\Delta Z_i + \Delta Z_{i+1}}{\frac{\Delta Z_i}{\rho_{p(i)} D_{AB(i)}} + \frac{\Delta Z_{i+1}}{\rho_{p(i+1)} D_{AB(i+1)}}} \quad (6)$$

The thermal conductivity of product  $k_p$ , product density  $\rho_p$  and diffusivity of liquid moisture  $D_{AB}$  are function of product moisture content and temperature which varies continuously at different depth of the drying product during drying.

Considering ideal and unidirectional shrinkage, the thickness of a particular control element is determine by moisture and solid balance of the control element as

$$\Delta Z_i^{t+\Delta t} = \frac{\rho_{m,i}^{t+\Delta t}}{\rho_w} \Delta Z_i^t + \frac{\Delta m_{solid,i}}{\rho_{solid} A} \quad (7)$$

The set of coupled non-linear Eq. (1) to (7) constitutes the governing equations that can be expressed in term of the two field variables  $T_p$  and  $\rho_m$ .

### 2.3 Initial Conditions

Initially the drying material is assumed to be at uniform temperature and moisture concentration, thus the initial conditions can be expressed as

$$\text{At time } t = 0 \text{ and } 0 \leq Z \leq H; T_p = T_{p,o}, \rho_m = \rho_{m,o}. \quad (8)$$

## 2.4 Boundary Conditions

If the drying product is placed on a solid insulated metal drying tray with which it maintains constant contact throughout the drying process without distortion, the boundary conditions for the bottom surface are:

$$\text{At time } t > 0 \text{ and } Z = 0; \quad \frac{\partial T_p}{\partial Z} = 0, \quad \frac{\partial \rho_m}{\partial Z} = 0 \quad (9)$$

If a heater of constant heat flux  $\dot{q}_{heater}$  is used to heat the product from the bottom as shown in Figure 1, the energy equation for the bottom control volume becomes

$$\frac{\partial T_p}{\partial t} \Big|_{i=1} = \frac{1}{(\Delta Z \rho_p C_p)_{(i=1)}} \left[ \dot{q}_{heater} + k_p \frac{\partial T_p}{\partial Z} \Big|_{i=1 \text{ to } 2} + \Delta Z Q_{mw} \Big|_{i=1} \right] \quad (10)$$

Evaporation of liquid moisture takes place at the drying surface. Thus, at time  $t > 0$  and  $Z = H$ ;

$$\frac{\partial \rho_m}{\partial t} \Big|_{i=n} = \frac{1}{\Delta Z_{i=n}} \left[ -(\rho_p D_{AB})_{(n-i \text{ to } n)} \frac{\partial \rho_m}{\partial Z} \Big|_{i=n \text{ to } n} - J_{m,s} \right] \quad (11)$$

where  $J_{m,s}$  is the mass flux of evaporated moisture from the drying surface, which can be determined from

$$J_{m,s} = h_m \left( \frac{M_w}{R} \right) \left[ \frac{A_w P_{v,sat \text{ at } T_{p,i=n}}}{T_{p,i=n}} - \frac{\phi P_{v,sat \text{ at } T_{air}}}{T_{air}} \right] \quad (12)$$

The mass transfer coefficient of vapor in the drying air  $h_m$  was calculated using the following empirical correlation [Saravacos & Maroulis, 2001]:

$$Sh = 0.664 Re^{0.5} Sc^{1/3} \quad (13)$$

Energy balance for the control volume at drying surface gives at time  $t > 0$  and  $Z = H$ ;

$$\frac{\partial T_p}{\partial t} \Big|_{i=n} = \frac{1}{(\Delta Z \rho_p C_p)_{(i=n)}} \left[ \dot{q}_{rad} + \dot{q}_{conv} - \dot{q}_{vapor} - k_p \frac{\partial T_p}{\partial Z} \Big|_{i=n \text{ to } n} + \Delta Z Q_{mw} \Big|_{i=n} \right] \quad (14)$$

where  $\dot{q}_{rad}$ ,  $\dot{q}_{conv}$  and  $\dot{q}_{vapor}$  are the radiation, convection and vapor heat flux, respectively, which can be expressed as

$$\dot{q}_{rad} = \varepsilon_p \sigma (T_{rad}^4 - T_{p,i=n}^4) \quad (15)$$

$$\dot{q}_{conv} = h_{air} (T_{air} - T_{p,i=n}) \quad (16)$$

$$\dot{q}_{vapor} = J_{m,s} h_{vap} \quad (17)$$

The convective air-to-product heat transfer coefficient  $h_{air}$  was calculated using the following correlation [Saravacos & Maroulis, 2001]:

$$Nu = 0.664 Re^{0.5} Pr^{1/3} \quad (18)$$

The total enthalpy for moisture vaporization  $h_{vap}$  can be expressed as

$$h_{vap} = h_{fg \text{ at } T_{p,i=n}} + \Delta H_w \quad (19)$$

where  $\Delta H_w$  is the heat of wetting, which increases significantly at lower moisture contents [Keey, 1972].

The thermodynamic and transport properties of air/water system and the physical properties of the potato sample are summarized in Table 1. The governing equations are solved simultaneously with appropriate boundary conditions using a 4<sup>th</sup> order Runge-Kutta scheme. A

MATLAB computer code was written to solve the governing equations, where the transport and physical properties are continuously updated in each time step of computing [Etter, 1993].

### **3. MATERIAL AND METHODS**

Fresh potato was purchased from the supermarket under the same brand name to ensure consistency of physical properties and used as the model material for the test. The average initial moisture content of six different samples was measured to be 4.6 kg/kg db. The drying rate of potato slices was measured in a heat pump dryer. The potato samples were skinned and sliced with an adjustable food-slicer to 5 mm thickness and cut to 30 mm by 30 mm with a twin-knife fixture. Twelve identical samples were placed on a tray, made of thin stainless steel plate, positioned in the drying chamber of the heat pump dryer and measured the variation of moisture content with drying time. Temperature and relative humidity of the drying air at the inlet and exit of the tray were measured using Omega Research type ‘T’ thermocouple probes and Vaisala digital electronic humidity transmitters. All thermocouples are calibrated using a master thermometer whose uncertainty is 0.05 °C. Vaisala factory, Finland, compared the output of the humidity transmitters for two values of factory working standard which showed the accuracy of  $\pm 0.75\%$ . Local velocity distribution over the tray was measured using a digital electronic hot bulb probe, whose accuracy is  $\pm (0.03 \text{ m/s} \pm 5\% \text{ of mV})$ . The weight of the specimen during drying was measured using a digital electronic balance, A&D, model GX-2000, of accuracy  $\pm 0.01\text{g}$  for a maximum weight of 2100 g. The outputs of the thermocouples, humidity transmitters, velocity probe and the weighing balance were recorded continuously in a data acquisition system.

### **4. RESULTS AND DISCUSSION**

#### **4.1 Verification of Model**

The variation of product mean moisture content with drying time was predicted using the liquid diffusion model and compared with the experimental results under the same drying condition as shown in Figure 2. The moisture content of the material was predicted for four different cases, which are:

- Case-A: No heat transfer by conduction through tray; product is an ideal shrinking material.
- Case-B: No heat transfer by conduction through tray; product is a non-shrinking material.
- Case-C: Heat transfer by conduction through tray; product is an ideal shrinking material.
- Case-D: Heat transfer by conduction through tray; product is a non-shrinking material.

When ideal shrinkage of the material was considered (case-A and C), which is more realistic in practical drying, the model predicted faster drying rate especially at low moisture contents in comparison with the experimental result as shown in Figure 2. As the material shrinks with decrease of its moisture content, the diffusion path for the liquid moisture to reach the drying surface for vaporization decreases. Consequently, moisture migrates from bulk to the drying surface of the material over shorter distances and over-predicts the moisture evaporation rate. In the present model moisture diffusivity is considered as a function only of temperature and moisture content. Above results show the logical need to include the effect of shrinkage in the moisture diffusivity correlation. As the samples were placed on a tray, made of thin stainless steel plate which was positioned in the drying chamber, heat was transferred from drying air to the bottom surface of the product through the tray, which was considered in case-B and D. Case-D showed good agreement between predicted moisture values and experimental data (Figure 2). The predicted drying rate of case-D is slightly lower than that of experimental result. As one-dimensional liquid diffusion was considered in the present model, moisture evaporated from the

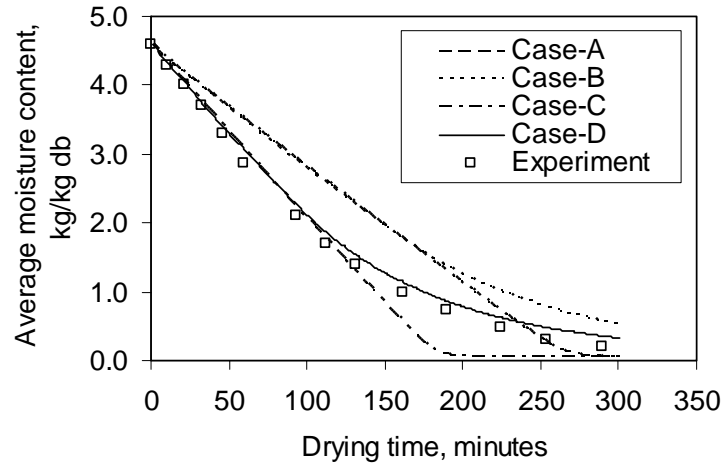


**Figure 2** Comparison between moisture content obtained from experimental data and simulation model. Graphs: Case-A: No conduction through tray, with shrinkage; Case-B: No conduction through tray, without shrinkage; Case-C: With conduction through tray, with shrinkage; Case-D: With conduction through tray, without shrinkage.

sidewalls of the material was neglected. With the decrease of moisture content, the material shrinks and the side wall area as well as evaporation from the sidewalls decreases. However, the material deforms at low moisture content. Consequently, bottom surface of the material, which was in contact to the tray, detaches and moisture evaporates from bottom surface as well which is not considered in the present simplified model.

#### 4.2 Cases Studied Using Diffusion Model

Table 2 summarizes the cases considered to investigate the drying performance using one dimensional diffusion model.

**Table 2** Cases studied using one dimensional diffusion model.  
(Model material: Potato slice; Initial moisture content: 4.6 kg/kg db.)

<b>Effect of shrinkage</b>	
Case-1	Mode of heat input: Convection; Drying air condition: $V_{\text{air}} = 2 \text{ m/s}$ , $T_{\text{air}} = 45 \text{ }^\circ\text{C}$ , $RH_{\text{air}} = 15\%$ ; Initial thickness of material = 5 mm; Shrinkage: Ideal shrinkage.
Case-2	Mode of heat input: Convection; Drying air condition: $V_{\text{air}} = 2 \text{ m/s}$ , $T_{\text{air}} = 45 \text{ }^\circ\text{C}$ , $RH_{\text{air}} = 15\%$ ; Initial thickness of material = 5 mm; Shrinkage: No shrinkage.
<b>Effect of different modes of heat input</b>	
Case-3	Modes of heat input: Convection and conduction; Drying air condition: $V_{\text{air}} = 2 \text{ m/s}$ , $T_{\text{air}} = 45 \text{ }^\circ\text{C}$ , $RH_{\text{air}} = 15\%$ ; Conduction heat flux: $500 \text{ W/m}^2$ ; Initial thickness of material = 5 mm; Shrinkage: No shrinkage.
Case-4	Modes of heat input: Convection and radiation; Drying air condition: $V_{\text{air}} = 2 \text{ m/s}$ , $T_{\text{air}} = 45 \text{ }^\circ\text{C}$ , $RH_{\text{air}} = 15\%$ ; Temperature of radiation heater: $110 \text{ }^\circ\text{C}$ ; Initial thickness of material = 5 mm; Shrinkage: No shrinkage.

**Table 2** Cases studied using one dimensional diffusion model (cont'd).

Case-5	Modes of heat input: Convection and Microwave; Drying air condition: $V_{\text{air}} = 2$ m/s, $T_{\text{air}} = 45$ °C, $RH_{\text{air}} = 15\%$ ; Microwave power: 0.6 W/g of initial wet material; Initial thickness of material = 5 mm; Shrinkage: No shrinkage.
<b>Effect of stepwise change of drying air temperature</b>	
Case-6	Temperature profile of drying air: Square wave-form Maximum air temperature: $T_{\text{air}} = 45$ °C with $RH_{\text{air}} = 15\%$ ; Minimum air temperature: $T_{\text{air}} = 30$ °C with $RH_{\text{air}} = 33.8\%$ ; Cycle time: 4 hours; Mode of heat input: Convection; Drying air condition: $V_{\text{air}} = 2$ m/s; Initial thickness of material = 5 mm; Shrinkage: No shrinkage.
Case-7	Temperature profile of drying air: Step down-form Maximum air temperature: $T_{\text{air}} = 45$ °C with $RH_{\text{air}} = 15\%$ ; Minimum air temperature: $T_{\text{air}} = 30$ °C with $RH_{\text{air}} = 33.8\%$ ; Time step size: 2 hours; Temperature step size: -5 °C; Mode of heat input: Convection; Drying air velocity: $V_{\text{air}} = 2$ m/s; Initial thickness of material = 5 mm; Shrinkage: No shrinkage.
Case-8	Temperature profile of drying air: Step up-form Minimum air temperature: $T_{\text{air}} = 30$ °C with $RH_{\text{air}} = 33.8\%$ ; Maximum air temperature: $T_{\text{air}} = 45$ °C with $RH_{\text{air}} = 15\%$ ; Time step size: 2 hours; Temperature step size: 5 °C; Mode of heat input: Convection; Drying air velocity: $V_{\text{air}} = 2$ m/s; Initial thickness of material = 5 mm; Shrinkage: No shrinkage.
Case-9	Temperature profile of drying air: Step down-form Maximum air temperature: $T_{\text{air}} = 65$ °C with $RH_{\text{air}} = 5.8\%$ ; Minimum air temperature: $T_{\text{air}} = 45$ °C with $RH_{\text{air}} = 15\%$ ; Temperature step size: -5 °C; Temperature controller: On/off type temperature controller is simulated to maintain maximum allowable product temperature of 45°C; Mode of heat input: Convection; Drying air velocity: $V_{\text{air}} = 2$ m/s; Initial thickness of material = 5 mm; Shrinkage: No shrinkage.
<b>Effect of stepwise change of drying air velocity</b>	
Case-10 (Base case)	Drying air velocity during drying process, $V_{\text{air}} = 2$ m/s; Drying air condition: $T_{\text{air}} = 45$ °C, $RH_{\text{air}} = 10\%$ ; Mode of heat input: Convection; Total drying time: 8 hours; Initial thickness of material = 5 mm; Shrinkage: No shrinkage.
Case-11	Drying air velocity during drying process, $V_{\text{air}} = 0.5$ m/s; Drying air condition: $T_{\text{air}} = 45$ °C, $RH_{\text{air}} = 10\%$ ; Mode of heat input: Convection; Total drying time: 8 hours; Initial thickness of material = 5 mm; Shrinkage: No shrinkage.
Case-12	Velocity profile of drying air: Step down-form Maximum air velocity: $V_{\text{air}} = 2$ m/s; Minimum air velocity: $V_{\text{air}} = 0.5$ m/s; Time step size: 2 hours; Velocity step size: -0.5 m/s; Drying air condition: $T_{\text{air}} = 45$ °C, $RH_{\text{air}} = 10\%$ ; Mode of heat input: Convection; Total drying time: 8 hours; Initial thickness of material = 5 mm; Shrinkage: No shrinkage.

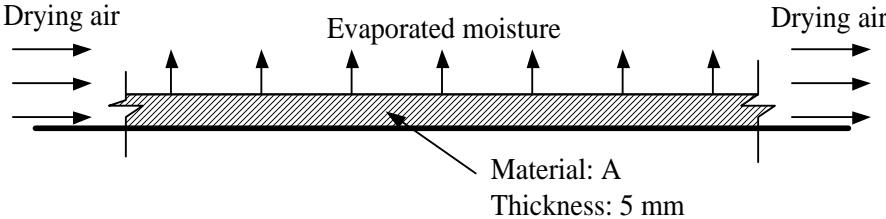
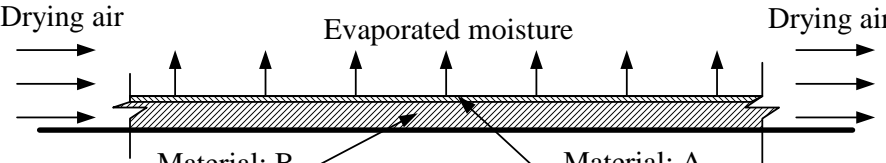
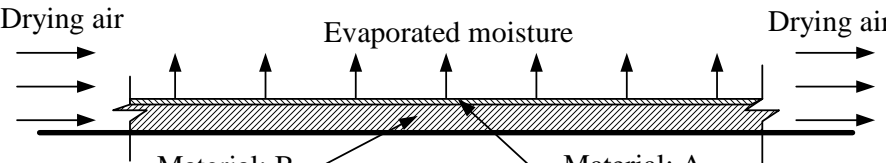
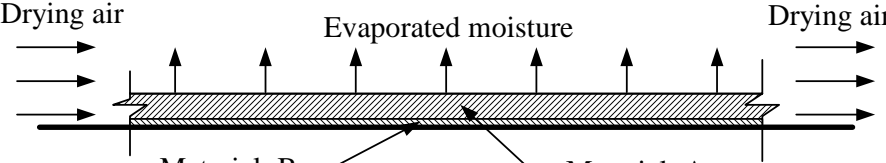
**Table 2** Cases studied using one dimensional diffusion model (cont'd).

Case-13	Velocity profile of drying air: Single step down-form $V_{\text{air}}$ is 2.0 m/s from 0 to 2 hours of drying process; $V_{\text{air}}$ is 0.5 m/s from 2 to 8 hours of drying process; Drying air condition: $T_{\text{air}} = 45\text{ }^{\circ}\text{C}$ , $\text{RH}_{\text{air}} = 10\%$ ; Mode of heat input: Convection; Total drying time: 8 hours; Initial thickness of material = 5 mm; Shrinkage: No shrinkage.
<b>Optimization of heat pump (HP)</b>	
Case-14 (Base case)	Mode of heat input: Convection; Heat Pump: Turned off during drying process; Drying air condition: $V_{\text{air}} = 2\text{ m/s}$ , $T_{\text{air}} = 45\text{ }^{\circ}\text{C}$ , $\text{RH}_{\text{air}} = 30\%$ ; Initial thickness of material = 5 mm; Shrinkage: No shrinkage.
Case-15	Mode of heat input: Convection; Heat Pump: Turned on during drying process; Drying air condition: $V_{\text{air}} = 2\text{ m/s}$ , $T_{\text{air}} = 45\text{ }^{\circ}\text{C}$ , $\text{RH}_{\text{air}} = 7\%$ ; Initial thickness of material = 5 mm; Shrinkage: No shrinkage.
Case-16	Mode of heat input: Convection; Heat Pump: Turned on with full capacity for 0 to 2 hours and with half capacity for 2 to 4 hours of drying process; Drying air condition: $V_{\text{air}} = 2\text{ m/s}$ , $T_{\text{air}} = 45\text{ }^{\circ}\text{C}$ ; $\text{RH}_{\text{air}}$ : 7% from 0 to 2 hours, 15% from 2 to 4 hours and 30% from 4 to 8 hours; Initial thickness of material = 5 mm; Shrinkage: No shrinkage.
Case-17	Mode of heat input: Convection; Heat Pump: Turned on with full capacity for 0 to 2 hours of drying process; Drying air condition: $V_{\text{air}} = 2\text{ m/s}$ , $T_{\text{air}} = 45\text{ }^{\circ}\text{C}$ ; $\text{RH}_{\text{air}}$ : 7% from 0 to 2 hours and 30% from 4 to 8 hours; Initial thickness of material = 5 mm; Shrinkage: No shrinkage.
<b>One heat pump (HP) for multiple drying chamber</b>	
Case-18 (Base case)	Mode of heat input: Convection; Number of drying chamber: 1 Heat pump is turned off continuously during drying process; Drying air condition: $V_{\text{air}} = 2\text{ m/s}$ , $T_{\text{air}} = 30\text{ }^{\circ}\text{C}$ , $\text{RH}_{\text{air}} = 67.75\%$ ; Initial thickness of material = 5 mm; Shrinkage: No shrinkage.
Case-19	Mode of heat input: Convection; Number of drying chamber: 1 Heat pump is turned on continuously during drying process; Drying air condition: $V_{\text{air}} = 2\text{ m/s}$ , $T_{\text{air}} = 45\text{ }^{\circ}\text{C}$ , $\text{RH}_{\text{air}} = 7\%$ ; Initial thickness of material = 5 mm; Shrinkage: No shrinkage.
Case-20	Mode of heat input: Convection; Number of drying chamber: 3 Heat pump is turned on continuously during drying process. Dehumidified hot air from the heat pump is supplied to the first drying chamber and atmospheric air is supplied to the other two drying chambers using a blower. The drying process is continued with the above drying conditions for 30 minutes. Dehumidified hot air from the heat pump is then switched to the next drying chamber while atmospheric air is supplied to the other two drying chambers. The cycle is repeated until the drying process is over. Drying air condition after heat pump: $V_{\text{air}} = 2\text{ m/s}$ , $T_{\text{air}} = 45\text{ }^{\circ}\text{C}$ , $\text{RH}_{\text{air}} = 7\%$ ; Drying air condition after air blower: $V_{\text{air}} = 2\text{ m/s}$ , $T_{\text{air}} = 30\text{ }^{\circ}\text{C}$ , $\text{RH}_{\text{air}} = 67.75\%$ ; Initial thickness of material = 5 mm; Shrinkage: No shrinkage.

**Table 2** Cases studied using one dimensional diffusion model (cont'd).

<b>Drying of product of low moisture diffusivity</b>	
Case-21	Moisture diffusivity of product = half of moisture diffusivity of potato Mode of heat input: Convection; Heat pump: Turned off during drying process Drying air condition: $V_{\text{air}} = 2 \text{ m/s}$ , $T_{\text{air}} = 45 \text{ }^\circ\text{C}$ , $\text{RH}_{\text{air}} = 30 \%$ ; Initial thickness of material = 5 mm; Shrinkage: No shrinkage.
Case-22	Moisture diffusivity of product = half of moisture diffusivity of potato Mode of heat input: Convection; Heat pump: Turned off during drying process Drying air condition: $V_{\text{air}} = 2 \text{ m/s}$ , $T_{\text{air}} = 35 \text{ }^\circ\text{C}$ , $\text{RH}_{\text{air}} = 51.1 \%$ ; Initial thickness of material = 5 mm; Shrinkage: No shrinkage.
Case-23	Moisture diffusivity of product = half of moisture diffusivity of potato Mode of heat input: Convection; Heat pump: Turned on during drying process Drying air condition: $V_{\text{air}} = 2 \text{ m/s}$ , $T_{\text{air}} = 45 \text{ }^\circ\text{C}$ , $\text{RH}_{\text{air}} = 7 \%$ ; Initial thickness of material = 5 mm; Shrinkage: No shrinkage.
Case-24	Moisture diffusivity of product = half of moisture diffusivity of potato Mode of heat input: Convection; Heat pump: Turned on during drying process Drying air condition: $V_{\text{air}} = 2 \text{ m/s}$ , $T_{\text{air}} = 35 \text{ }^\circ\text{C}$ , $\text{RH}_{\text{air}} = 11.9 \%$ ; Initial thickness of material = 5 mm; Shrinkage: No shrinkage.
<b>Drying of product of high moisture diffusivity</b>	
Case-25	Moisture diffusivity of product = double of moisture diffusivity of potato Mode of heat input: Convection; Heat pump: Turned off during drying process Drying air condition: $V_{\text{air}} = 2 \text{ m/s}$ , $T_{\text{air}} = 45 \text{ }^\circ\text{C}$ , $\text{RH}_{\text{air}} = 30 \%$ ; Initial thickness of material = 5 mm; Shrinkage: No shrinkage.
Case-26	Moisture diffusivity of product = double of moisture diffusivity of potato Mode of heat input: Convection; Heat pump: Turned off during drying process Drying air condition: $V_{\text{air}} = 2 \text{ m/s}$ , $T_{\text{air}} = 35 \text{ }^\circ\text{C}$ , $\text{RH}_{\text{air}} = 51.1 \%$ ; Initial thickness of material = 5 mm; Shrinkage: No shrinkage.
Case-27	Moisture diffusivity of product = double of moisture diffusivity of potato Mode of heat input: Convection; Heat pump: Turned on during drying process Drying air condition: $V_{\text{air}} = 2 \text{ m/s}$ , $T_{\text{air}} = 45 \text{ }^\circ\text{C}$ , $\text{RH}_{\text{air}} = 7 \%$ ; Initial thickness of material = 5 mm; Shrinkage: No shrinkage.
Case-28	Moisture diffusivity of product = double of moisture diffusivity of potato Mode of heat input: Convection; Heat pump: Turned on during drying process Drying air condition: $V_{\text{air}} = 2 \text{ m/s}$ , $T_{\text{air}} = 35 \text{ }^\circ\text{C}$ , $\text{RH}_{\text{air}} = 11.9 \%$ ; Initial thickness of material = 5 mm; Shrinkage: No shrinkage.
<b>Drying of composite slabs of different moisture diffusivities</b>	
Case-29 (Base case)	Moisture diffusivity: Uniform through out the product Mode of heat input: Convection; Drying air condition: $V_{\text{air}} = 2 \text{ m/s}$ , $T_{\text{air}} = 45 \text{ }^\circ\text{C}$ , $\text{RH}_{\text{air}} = 15\%$ ; Drying time = 8hrs; Initial thickness of material = 5 mm; No shrinkage.

**Table 2** Cases studied using one dimensional diffusion model (cont'd).

Case-29 (cont,d)	 <p style="text-align: center;">Material: A Thickness: 5 mm</p>
Case-30	<p>Moisture diffusivity: Exposed layer is thinner but with higher diffusivity;            Mode of heat input: Convection;            Drying air condition: <math>V_{\text{air}} = 2 \text{ m/s}</math>, <math>T_{\text{air}} = 45 \text{ }^\circ\text{C}</math>, <math>RH_{\text{air}} = 15\%</math>;            Drying time = 8hrs; Initial thickness of material = 5 mm; No shrinkage.</p>  <p style="text-align: center;">Material: B Thickness: 4.25 mm Diffusivity: <math>D_B</math></p> <p style="text-align: center;">Material: A Thickness: 0.75 mm Diffusivity: <math>D_A</math> <math>D_A = 10 D_B</math></p>
Case-31	<p>Moisture diffusivity: Exposed layer is thinner but with lower diffusivity;            Mode of heat input: Convection;            Drying air condition: <math>V_{\text{air}} = 2 \text{ m/s}</math>, <math>T_{\text{air}} = 45 \text{ }^\circ\text{C}</math>, <math>RH_{\text{air}} = 15\%</math>;            Drying time = 8hrs; Initial thickness of material = 5 mm; No shrinkage.</p>  <p style="text-align: center;">Material: B Thickness: 4.25 mm Diffusivity: <math>D_B</math></p> <p style="text-align: center;">Material: A Thickness: 0.75 mm Diffusivity: <math>D_A</math> <math>D_A = 0.1 D_B</math></p>
Case-32	<p>Moisture diffusivity: Thick exposed layer of higher diffusivity;            Mode of heat input: Convection;            Drying air condition: <math>V_{\text{air}} = 2 \text{ m/s}</math>, <math>T_{\text{air}} = 45 \text{ }^\circ\text{C}</math>, <math>RH_{\text{air}} = 15\%</math>;            Drying time = 8hrs; Initial thickness of material = 5 mm; No shrinkage.</p>  <p style="text-align: center;">Material: B Thickness: 0.75 mm Diffusivity: <math>D_B</math></p> <p style="text-align: center;">Material: A Thickness: 4.25 mm Diffusivity: <math>D_A</math> <math>D_B = 0.1 D_A</math></p>

**Table 2** Cases studied using one dimensional diffusion model (cont'd).

<b>Effect of flipping of product</b>	
Case-33 (Base case)	Without flipping of product Mode of heat input: Convection; Drying air condition: $V_{\text{air}} = 2 \text{ m/s}$ , $T_{\text{air}} = 45 \text{ }^\circ\text{C}$ , $\text{RH}_{\text{air}} = 10\%$ ; Initial thickness of material = 10 mm; Shrinkage: No shrinkage.
Case-34	Product is flipped after every 1 hrs of drying; Mode of heat input: Convection; Drying air condition: $V_{\text{air}} = 2 \text{ m/s}$ , $T_{\text{air}} = 45 \text{ }^\circ\text{C}$ , $\text{RH}_{\text{air}} = 10\%$ ; Initial thickness of material = 10 mm; Shrinkage: No shrinkage.
<b>Sun drying</b>	
Case-35 (Base case)	Mode of heat input: Convection; Drying air condition: $V_{\text{air}} = 2 \text{ m/s}$ , $T_{\text{air}} = 45 \text{ }^\circ\text{C}$ , $\text{RH}_{\text{air}} = 30\%$ ; Initial thickness of material = 5 mm; Shrinkage: No shrinkage.
Case-36	Mode of heat input: Solar radiation Location: Singapore, Month: October, Time: 7.00 am to 7.00 pm Initial thickness of material = 5 mm; Shrinkage: No shrinkage.

#### 4.2.1 Effect of Shrinkage

- The predicted moisture distributions across the product thickness during drying by pure convection are shown in Figure 3.
- Evaporation of liquid moisture takes place from the product surface by absorbing the heat of vaporization as well as heat of desorption when removing bound moisture. As the initial moisture content at the drying surface of the product is high, it can evaporate rapidly at the beginning of the drying process. External mass transfer rate of vapor (external transport limitation) and the heat transfer rate to the product surface control the evaporation rate at this stage of drying. With diminishing surface moisture content, the evaporation rate is controlled by internal mass transfer rate of liquid moisture.
- It is worthwhile to note that the drop of internal moisture content is mainly confined in the region of the drying surface and slowly progresses to the interior (Figure 3), because of the low moisture diffusivity of the product.

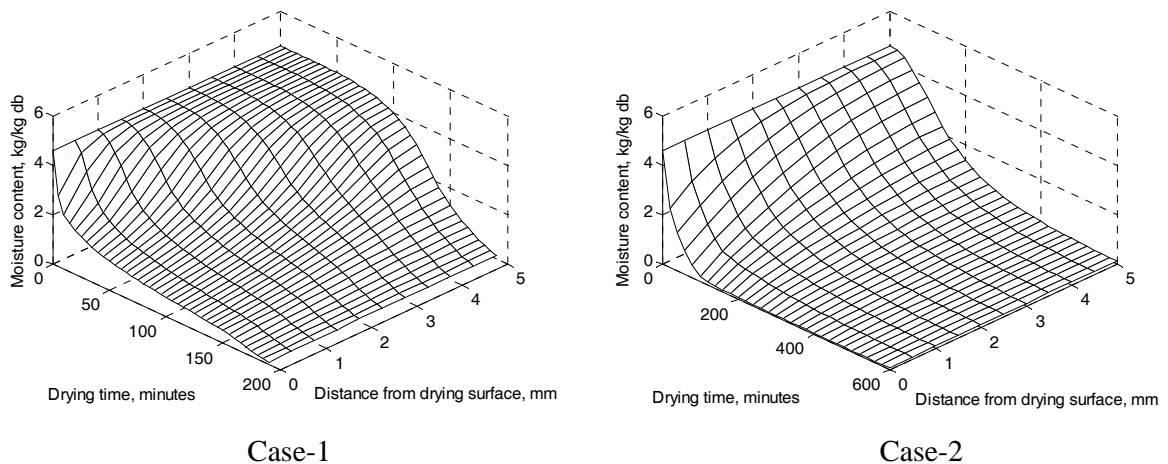


**Figure 3** Moisture distribution across the product during drying using pure convection. Case-1: with ideal shrinkage. Case-2: without shrinkage.

- For case-1 (ideal shrinkage), the diffusion path for the liquid moisture to reach the drying surface decreases with drying time. As a result the evaporation rate improves in comparison with that of the case-2 (non-shrinking) provided the water diffusivity remains unchanged, as is assumed in this study.
- Figure 4 shows that the temperature of the product drops sharply at the beginning of drying process. The sharp drop of product temperature indicates that the heat convected from the drying air to the product surface can not sustain the higher evaporation rate of moisture during the initial period of drying. The evaporating moisture takes the remaining heat as sensible heat from the product itself resulting in a sharp drop of product temperature.

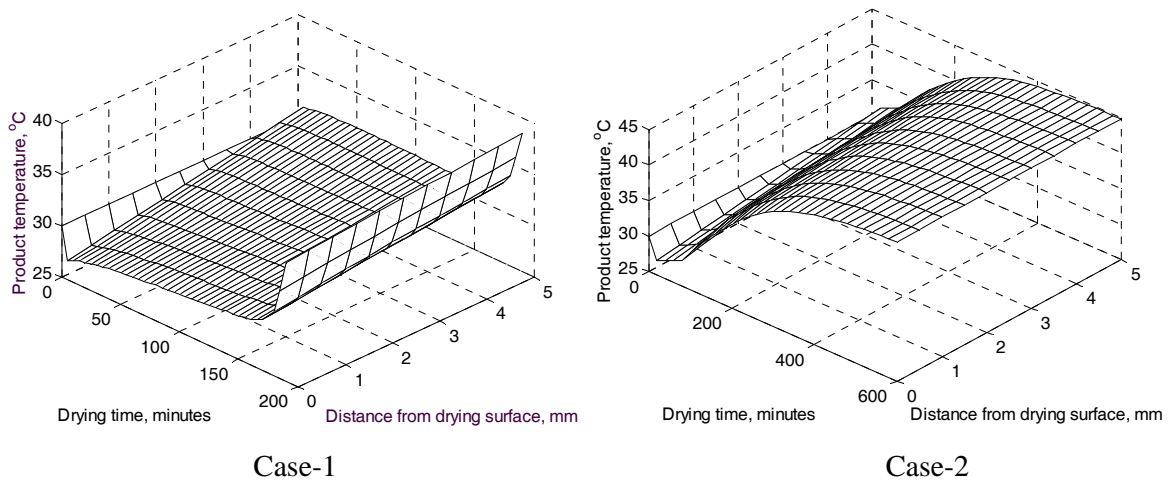


**Figure 4** Temperature distribution across the product during drying using pure convection. Case-1: with ideal shrinkage. Case-2: without shrinkage.

- After the initial drying period, the evaporation rate is controlled by moisture diffusion rate from the bulk to the surface of product as well as the temperature and moisture content at the surface that controls surface vapor pressure. During this period of drying, the temperature of the drying surface increases slowly (Figure 4) indicating the period of first falling rate.
- For case-1 (ideal shrinkage), product temperature remains low for longer period because of higher vaporization rate in comparison with that of case-2 (without shrinkage).
- As the flux of moisture decreases with drying time during this period of first falling rate, the energy transfer by convection becomes sufficient to supply the heat of vaporization and to heat up the product. Near the end of the drying process, the second falling rate starts which further drops the flux of moisture. Consequently, product temperature increases rapidly even though the heat of wetting increases exponentially during this period.
- It is important to note that unlike moisture, product temperature distribution is almost uniform throughout the product at a specific time in the drying process because of its low Biot number.
- Percentage shrinkage of control elements at different depth of the product during drying (for case-1) is shown Figure 5. As mentioned earlier, the drop of internal moisture content is mainly confined in the region of the drying surface and slowly progresses to the interior. The product shrinks following the same pattern because of the consideration of ideal shrinkage.
- The variation of the flux of moisture with average moisture content of the product for case-1 and 2 is shown in Figure 6. For moisture contents up to 0.5 kg/kg db, the flux of moisture

remains relatively high for case-1 (ideal shrinkage). First and second falling rate are more obvious for case-2 (without shrinkage).

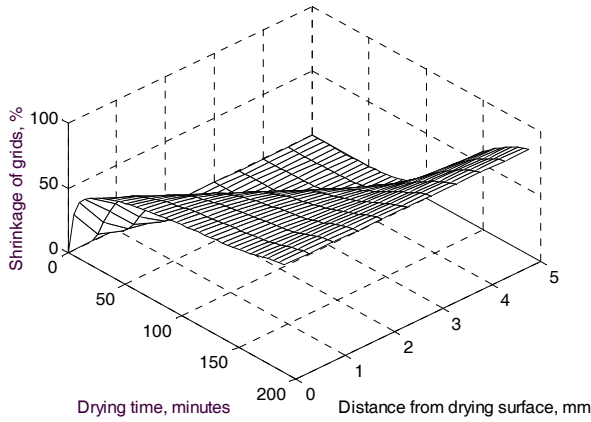


**Figure 5** Predicted shrinkage at different depths of product during drying

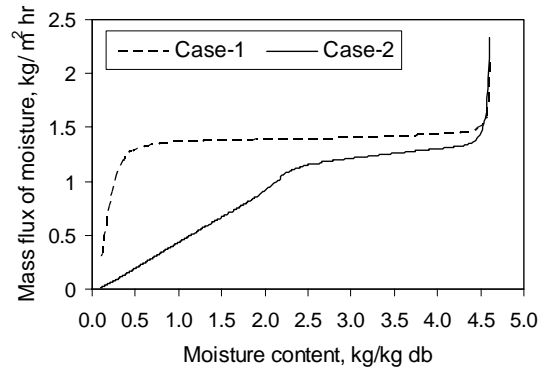


**Figure 6** Variation of moisture flux with average moisture content for convection drying. Case-1: with ideal shrinkage; Case-2: without shrinkage.

- Thermal conductivity and moisture diffusivity are both dependent on local temperature and moisture content of the product. During drying process, the distribution of thermal conductivity and moisture diffusivity inside the product are depicted in Figure 7 and 8.
- Both thermal conductivity and moisture diffusivity are small at the drying surface because of low moisture content.

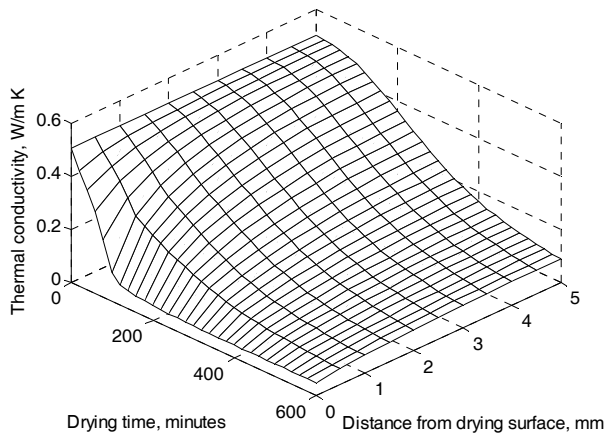


**Figure 7** Variation of thermal conductivity across the product during drying using pure convection (Case-2: without shrinkage).

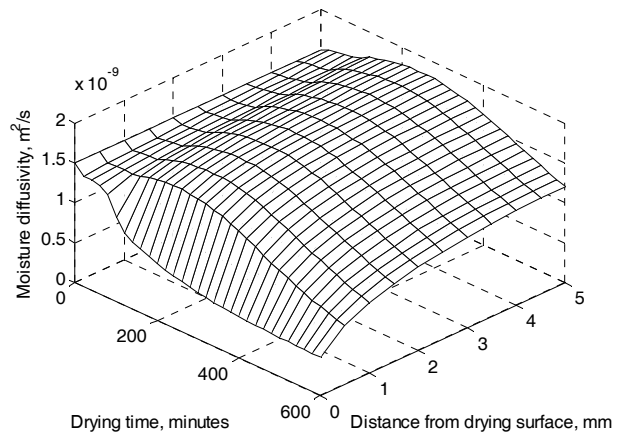
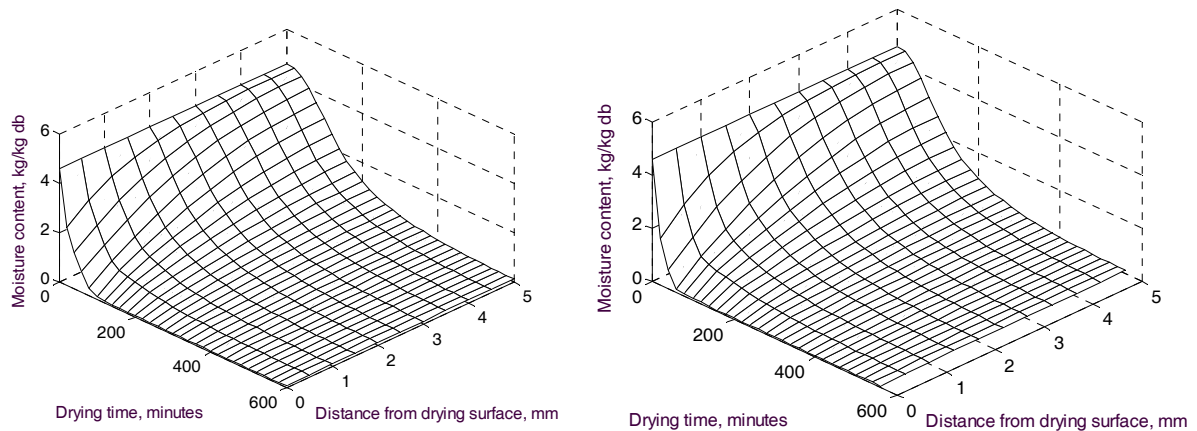


**Figure 8** Variation of moisture diffusivity across the product during drying using pure convection (Case-2: without shrinkage).

#### 4.2.2 Effect of Different Modes of Heat Input

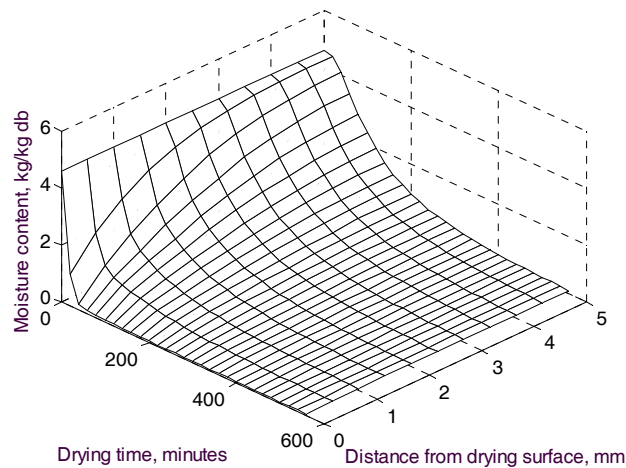
- The distributions of moisture content throughout the product for different modes of heat input which include convection combined with conduction, radiation and volumetric heating using microwave field are shown in Figure 9.

- As the evaporation of moisture takes place from the drying surface of the product, moisture content drops rapidly at the drying surface and then slowly progress to the interior for all modes of drying. Although the moisture distribution patterns are very similar for different modes of heat input, the drying times required to reach the moisture content from 4.6 kg/kg db to 0.1 kg/kg db are different. Diffusivity of moisture depends on product temperature and moisture content. Microwave energy generates heat internally in the product and maintains relatively higher temperature throughout the product. Consequent, for the same moisture content, diffusivity of moisture becomes higher and the drying time becomes shorter for the input of microwave energy in comparison with that of the other modes of heat input.
- Drying time will change with the change of intensity of the input powers.



Case-3

Case-4



Case-5

**Figure 9** Moisture distribution across the product during drying. Case-3: convection and conduction, Case-4: convection and radiation, Case-5: convection and microwave.

- Temperature distributions throughout the product for different modes of heat (convection combined with conduction, radiation and volumetric heating using microwave field) are shown in Figure 10.

- An on/off type temperature controller was simulated in the simulation program to predict control strategy for the power of the heaters and thereby maintain the product temperature always within the range 40 to 45°C to avoid degradation of quality.
- The on/off sequences of the heaters under different modes of drying are reflected in the product temperatures as shown in Figure 10.
- For case-4 (convection and radiation), product temperature becomes maximum at the drying surface because the radiation heat is supplied to the drying surface.
- For case-3 (convection and conduction) and 5 (convection and microwave), product temperature becomes maximum at the bottom surface. For case-3, radiation heat is supplied from the bottom of the product. Microwave generates more heat in the bottom region of the product because of its higher moisture content.

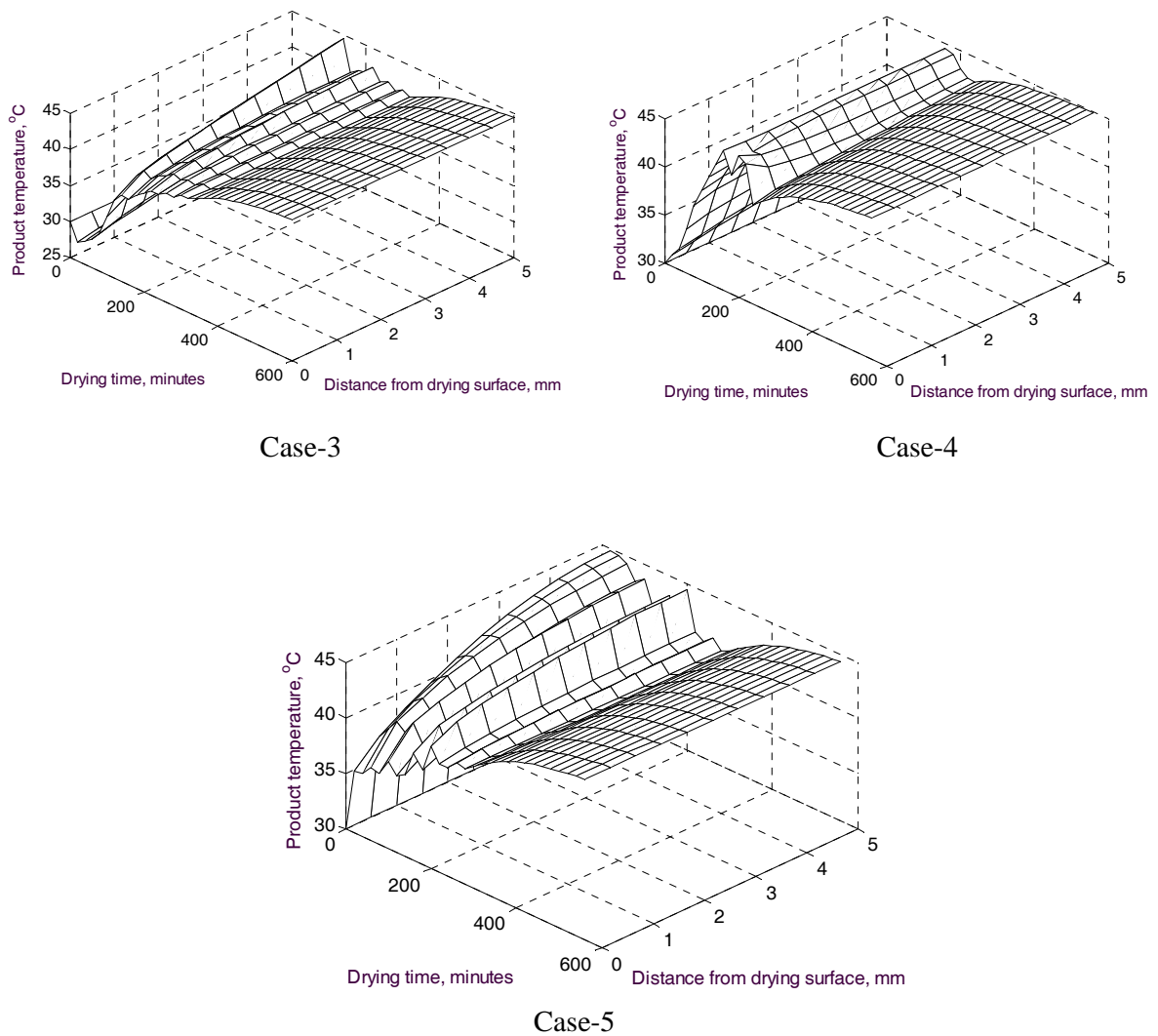


**Figure 10** Temperature distribution across the product during drying. Case-3: convection and conduction, Case-4: convection and radiation, Case-5: convection and microwave.

- The variation of the flux of moisture with average moisture content of the product using different modes of heat transfer (case-1 to 5) is shown in Figure 11.

- The variation of average moisture content of the product with drying time for case-1 to 5 is shown in Figure 12.
- Combination of different modes of heat input increase moisture flux up to moisture content of about 2.5 kg/kg db.
- For moisture content lower than 2.5 kg/kg db, the evaporation rate is controlled by internal mass transfer rate of liquid moisture and the effect of different modes of heat input diminishes.

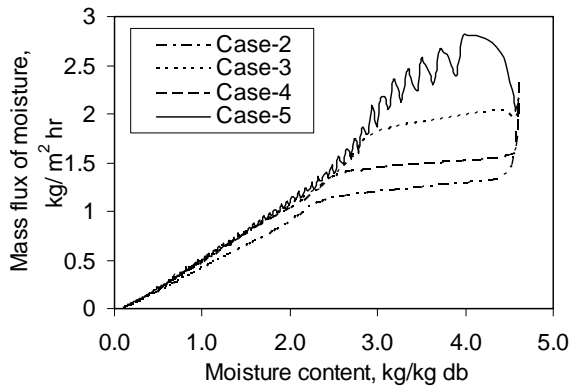


**Figure 11** Variation of moisture flux with average moisture content for different modes of heat input. Case-2: pure convection, Case-3: convection and conduction, Case-4: convection and radiation, Case-5: convection and microwave.

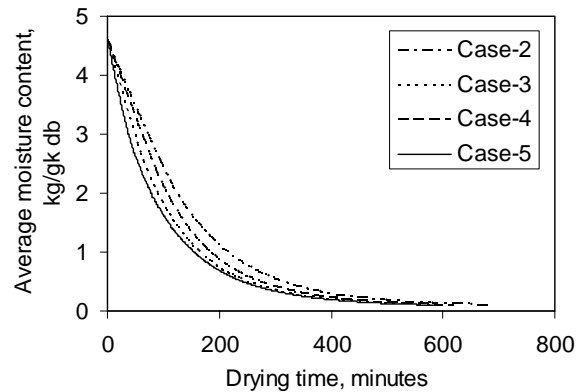
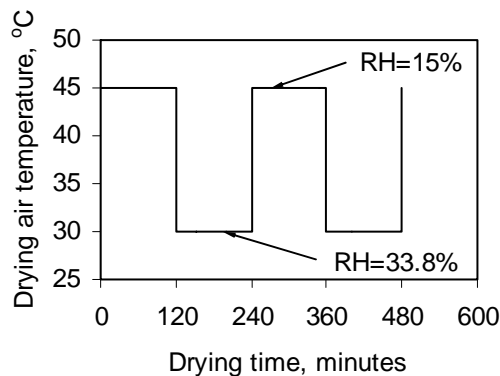


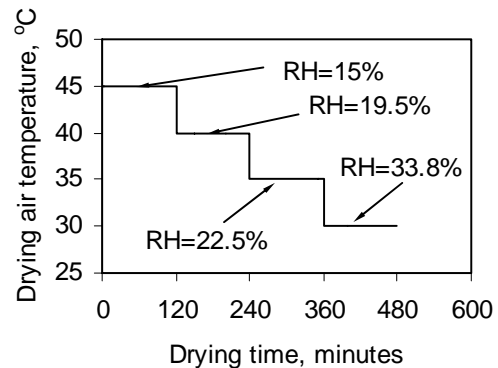
**Figure 12** Variation of average moisture content with drying time for different modes of heat input. Case-2: pure convection, Case-3: convection and conduction, Case-4: convection and radiation, Case-5: convection and microwave.

#### 4.2.3 Effect of Stepwise Change of Drying Air Temperature

- Different profiles of stepwise change of drying air temperature considered in the study are shown in Figure 13.
- For case-9, drying air temperature is controlled to maintain the maximum allowable temperature of the product.
- Relative humidity of the drying air changes (keeping absolute humidity constant) because of the change of its temperature.

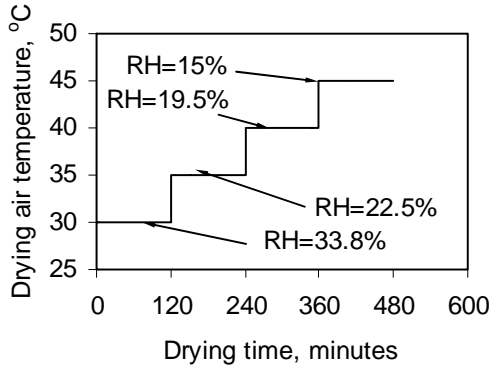


Case-6: Square wave-form

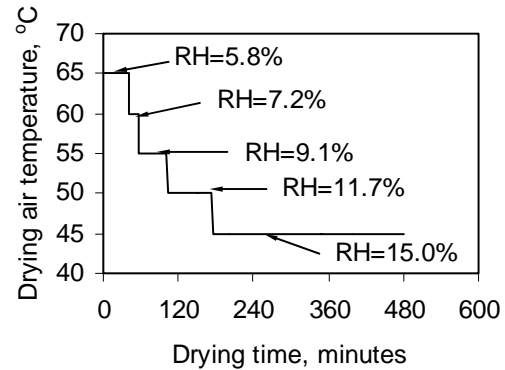


Case-7: Step-down profile

**Figure 13** Different profiles of stepwise change of drying air temperature.



Case-8: Step-up profile



Case-9: Unequal step-down profile

**Figure 13** Different profiles of stepwise change of drying air temperature (cont'd).

- Variation of inner and drying surface temperatures for stepwise changes of drying air temperature are shown in Figure 14 and 15, respectively.

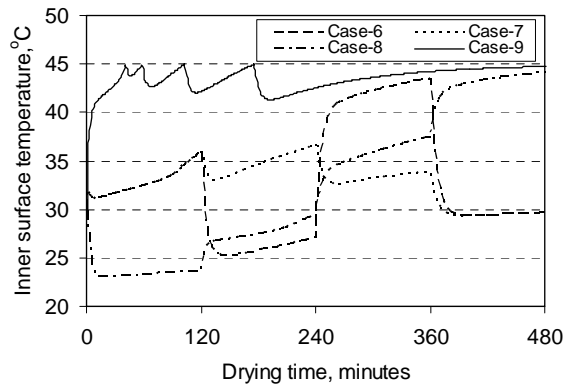


**Figure 14** Variation of inner surface temperature for stepwise changes of drying air temperature.

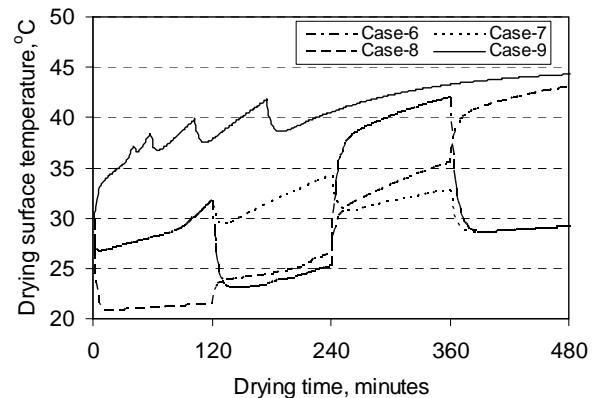


**Figure 15** Variation of drying surface temperature for stepwise changes of drying air temperature.

- Stepwise changes of drying air temperatures are reflected in the product temperatures.
- As moisture evaporates from the drying surface by absorbing heat of vaporization, drying surface temperatures become lower than that of inner surface.
- Higher temperature of drying air could be used in the initial period of drying.
- The variation of the flux of moisture with average moisture content of the product for stepwise changes of drying air temperatures (case-6 to 9) is shown in Figure 16.
- The variation of average moisture content of the product with drying time for case-6 to 9 is shown in Figure 17.
- Stepwise changes of drying air temperatures increase moisture flux up to moisture content of about 2.5 kg/kg db.

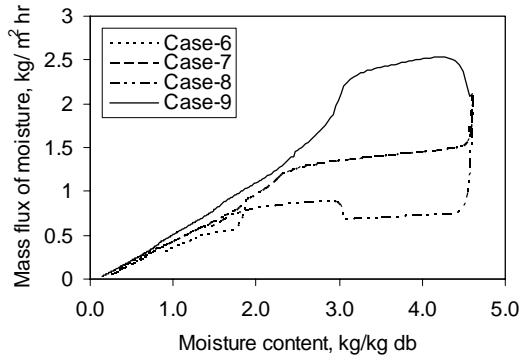


**Figure 16** Variation of moisture flux with average moisture content for stepwise changes of drying air temperatures.

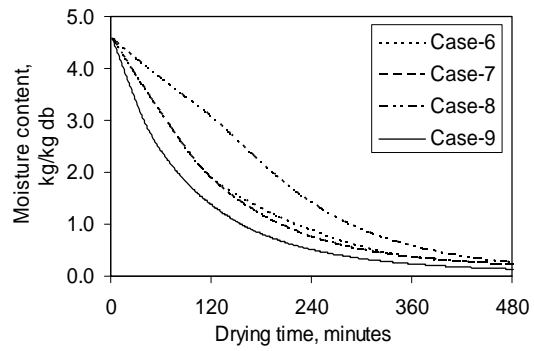


**Figure 17** Variation of average moisture content with drying time for different modes of heat input.

#### 4.2.4 Effect of Stepwise Change of Drying Air Velocity

- Convection heat and mass transfer coefficients between the drying surface of the product and the drying air depend on the air flow velocity. Case-10 to 13 was simulated to study the effect of the air flow velocity in the drying process.
- Figure 18 shows the variation of predicted mass flux of moisture with average moisture content of the product due to the change of drying air velocity (case-10 to 13). The variation of average moisture content of the product with drying time is shown in Figure 19.
- Figs. 18 and 19 show that case-10 (constant air velocity of 2 m/s) and case-12 (air velocity gradually decrease from 2 m/s to 0.5 m/s) give almost same drying performance. However, power consumption of blower for case-12 is half of case-10. Moreover, case-13 shows that blower should run at higher capacity only in the initial period of drying.

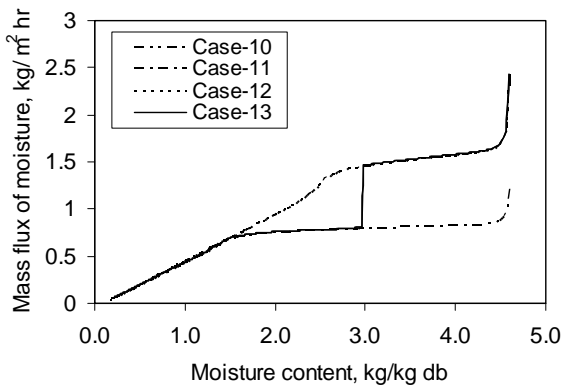


**Figure 18** Variation of moisture flux with average moisture content due to the change of drying air velocity.

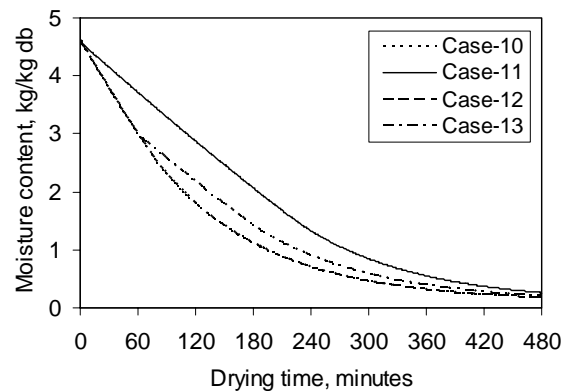


**Figure 19** Variation of average moisture content with drying time due to the change of drying air velocity.

#### 4.2.5 Optimization of Heat Pump (HP)

- Heat pump is used to control the relative humidity (RH) of the drying air. To study the effect of the relative humidity in the drying process, the following cases were studied:

- Case-14: heat pump is turned off; RH is 30 % from 0 to 8 hours of drying.
- Case-15: heat pump is turned on; RH is 7 % from 0 to 8 hours of drying.
- Case-16: power of heat pump is controlled; RH is 7 % from 0 to 2 hours, 15 % from 2 to 4 hours, and 30 % from 4 to 8 hours of drying.
- Case-17: power of heat pump is controlled; RH is 7 % from 0 to 2 hours and 30 % from 2 to 8 hours of drying.

- The variation of the flux of moisture with average moisture content of the product due to the change of drying air relative humidity (case-14 to 17) is shown in Figure 20.
- The variation of average moisture content of the product with drying time for case-14 to 17 is shown in Figure 21.
- Figs. 20 and 21 show that heat pump should be turned on only in the initial period of drying.

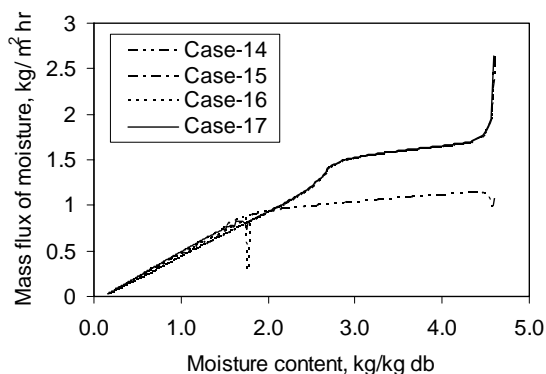


**Figure 20** Variation of moisture flux with average moisture content due to the change of drying air relative humidity.

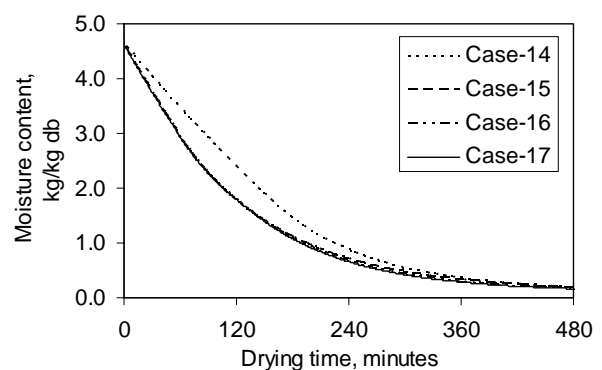


**Figure 21** Variation of average moisture content with drying time due to the change of drying air relative humidity.

#### 4.2.6 One Heat Pump (HP) for Multiple Drying Chambers

- Previous discussion shows that heat pump should not be turned on for the entire period of drying to minimize the running cost. A dryer with multiple drying chambers could be designed where only one heat pump will serve for all drying chambers. The optimum number of drying chambers that can be served by a single heat pump depends on the properties of the drying products. The simulation results for serving three drying chambers using one heat pump (case-18 to 20) is presented in Figure 22 and 23.
- Capital cost as well as operating cost can be reduced significantly. Depending on the properties of the product to be dried, optimum switching time of heat pump can be determined.
- Figure 23 shows that the effect of heat pump gradually becomes less significant at low moisture content of the product. Therefore, switching of heat pump is not even required near the end of the drying processes and the heat pump can be turned off.

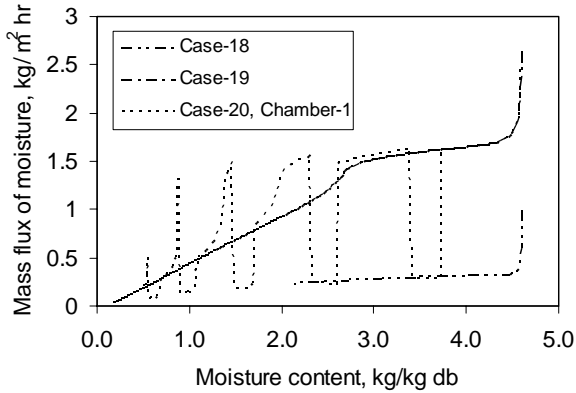


**Figure 22** Variation of moisture flux with average moisture content due to the change of drying air temperature, relative humidity and switching of heat pump.

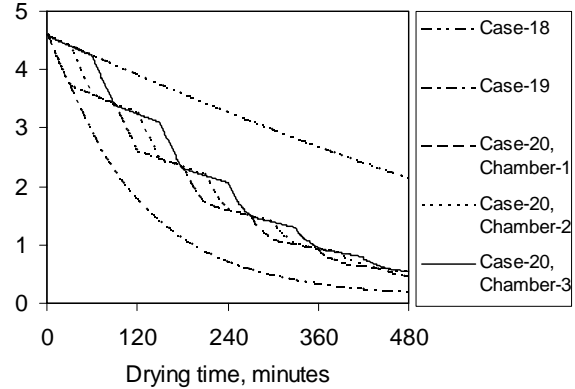


**Figure 23** Variation of average moisture content with drying time due to the change of drying air temperature, relative humidity and switching of heat pump.

#### 4.2.7 Drying of Product of Low Moisture Diffusivity

- To study the effect of drying air temperature and relative humidity on the drying performance of the products of relatively low moisture diffusivity, the diffusivity value used in the simulation was reduced to half of that of the potato. The following cases were studied:
  - Case-21: heat pump is turned off; drying air temperature is 45 °C and RH is 30 %.
  - Case-22: heat pump is turned off; drying air temperature is 35 °C and RH is 51.1 % (absolute humidity of case-21 and 22 is constant).
  - Case-23: heat pump is turned on; drying air temperature is 45 °C and RH is 7 %.
  - Case-24: heat pump is turned on; drying air temperature is 35°C and RH is 11.9 % (absolute humidity of case-23 and 24 is constant).
- The variation of the flux of moisture with average moisture content for the product of low diffusivity is shown in Figure 24.
- The variation of average moisture content of the product with drying time is shown in Figure 25.

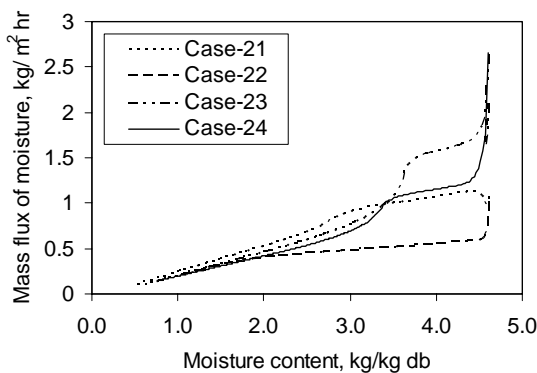


**Figure 24** Variation of moisture flux with average moisture content for products of low moisture diffusivity.

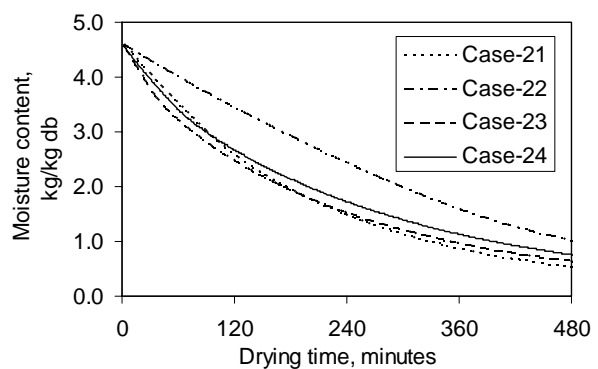


**Figure 25** Variation of average moisture content with drying time for products of low moisture diffusivity.

- As expected drying rate improves with the increase of temperature and decrease of relative humidity of the drying air.

- Figure 25 shows that drying rate for case-21 (Air temperature is 45 °C and relative humidity is 30%) is higher than that of case-23 (Air temperature is 45 °C and relative humidity is 7%). In the initial period of drying, moisture evaporation rate was higher for case-23 because of lower relative humidity of the drying air. However, because of the use of lower relative humidity of the drying air, surface of the product quickly becomes more dry which reduces diffusivity at the drying surface significantly and drops the drying rate for the remaining period of time.

#### 4.2.8 Drying of Product of High Moisture Diffusivity

- The diffusivity of the product sample was increased to double of the diffusivity of potato in the simulation to study the effect of drying air temperature and relative humidity on the drying performance of the products of high diffusivity.
- Drying conditions of case-25 to 28 are the same as that of case-21 to 24, respectively. However, the diffusivity value of the product is considered as double of the diffusivity of potato.
- The variation of the flux of moisture with average moisture content for the product of high diffusivity (case-25 to 28) is shown in Figure 26.
- The variation of average moisture content of the product with drying time is shown in Figure 27.

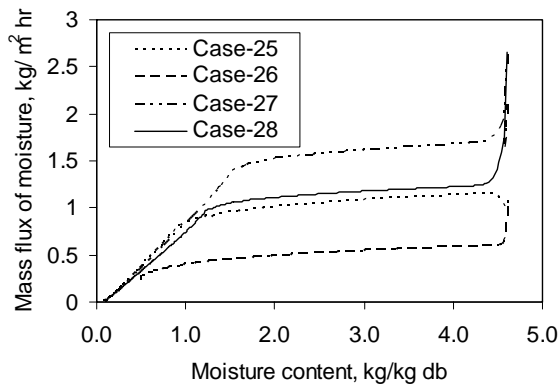


**Figure 26** Variation of moisture flux with average moisture content for products of high diffusivity.

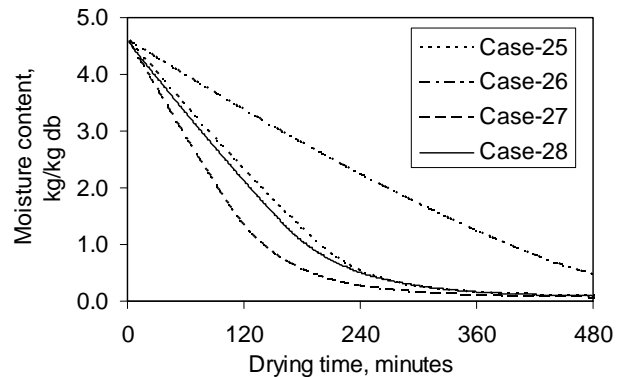


**Figure 27** Variation of average moisture content with drying time for products of high diffusivity.

- Because of high moisture diffusivity of the product, moisture can rapidly diffuse from bulk to the drying surface of the product and evaporation rate increases with the increase of temperature and decrease of relative humidity of the drying air.
- For high moisture diffusivity of the product, evaporation rate largely depends on the external drying conditions (externally controlled drying). Therefore, heat pump can increase drying rate significantly by reducing relative humidity of the drying air.

#### 4.2.9 Drying of Composite Slabs

- Drying of two-layer slabs with each layer of different thickness and moisture diffusivities was simulated (case-29 to 32). The variation of the mass flux of moisture with average moisture content and the average moisture content with drying time are shown in Figure 28 and 29, respectively.
- If the drying surface of the product dry quickly during drying process, the diffusivity of the drying surface may drop significantly this may hinder the overall drying rate. The above

mentioned problem could be minimized by exposing the layer of higher diffusivity of a composite slab to the drying air as shown in case-30.

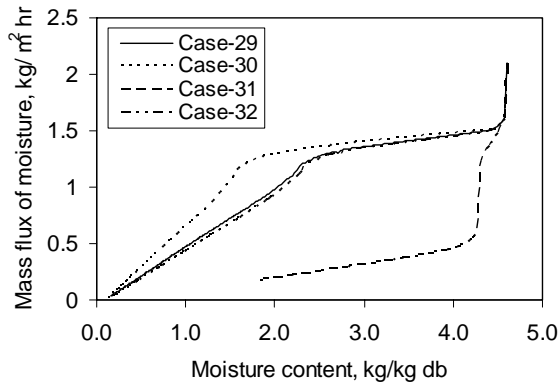


**Figure 28** Variation of moisture flux with average moisture content for composite materials of different moisture diffusivities.

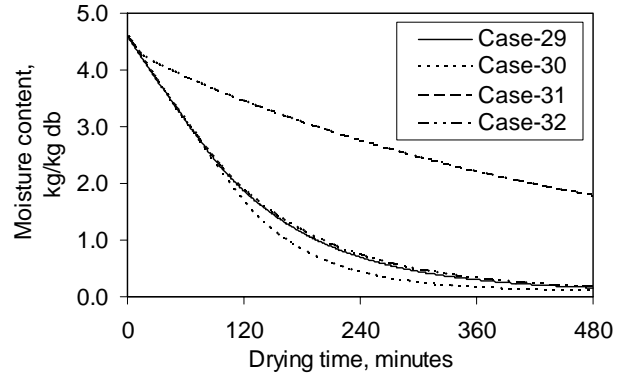


**Figure 29** Variation of average moisture content with drying time for composite materials of different moisture diffusivities.

- If a thin layer of low diffusivity is exposed to the drying air and works as the drying surface (case-31), the layer acts like a “skin” and the drying rate drops significantly. To avoid this situation, the thin layer of low diffusivity should be placed in the opposite way as shown in case-32.

#### 4.2.10 Effect of Flipping of Product

- To study the effect of flipping, the product is flipped after every 1 hour of drying.
- The variation of the flux of moisture with average moisture content of the product for case-33 (without flipping) and case-34 (with flipping) is shown in Figure 30.
- The variation of average moisture content of the product with drying time for case-33 to 34 is shown in Figure 31.

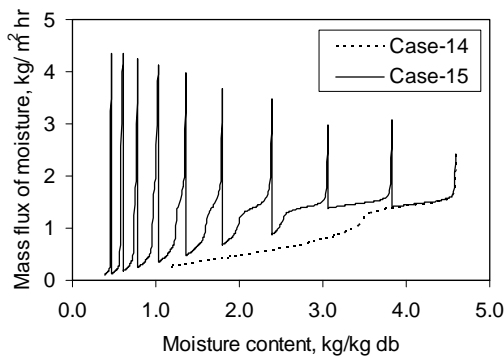


**Figure 30** Variation of moisture flux with average moisture content due to flipping

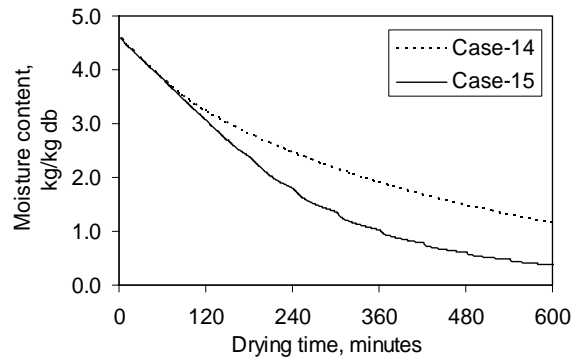


**Figure 31** Variation of average moisture content with drying time due to flipping

- Flipping of product improves drying performance.
- Effect of flipping reduces with decreasing of moisture content.

#### 4.2.11 Sun Drying

- Meteorological data for Singapore is used to simulate the drying process (Hawlder et al, 1990).
- Month: October; Drying time: 7.00 am to 7.00 pm.
- Variation of global radiation, air temperature, air relative humidity and air velocity is shown in Figure 32.

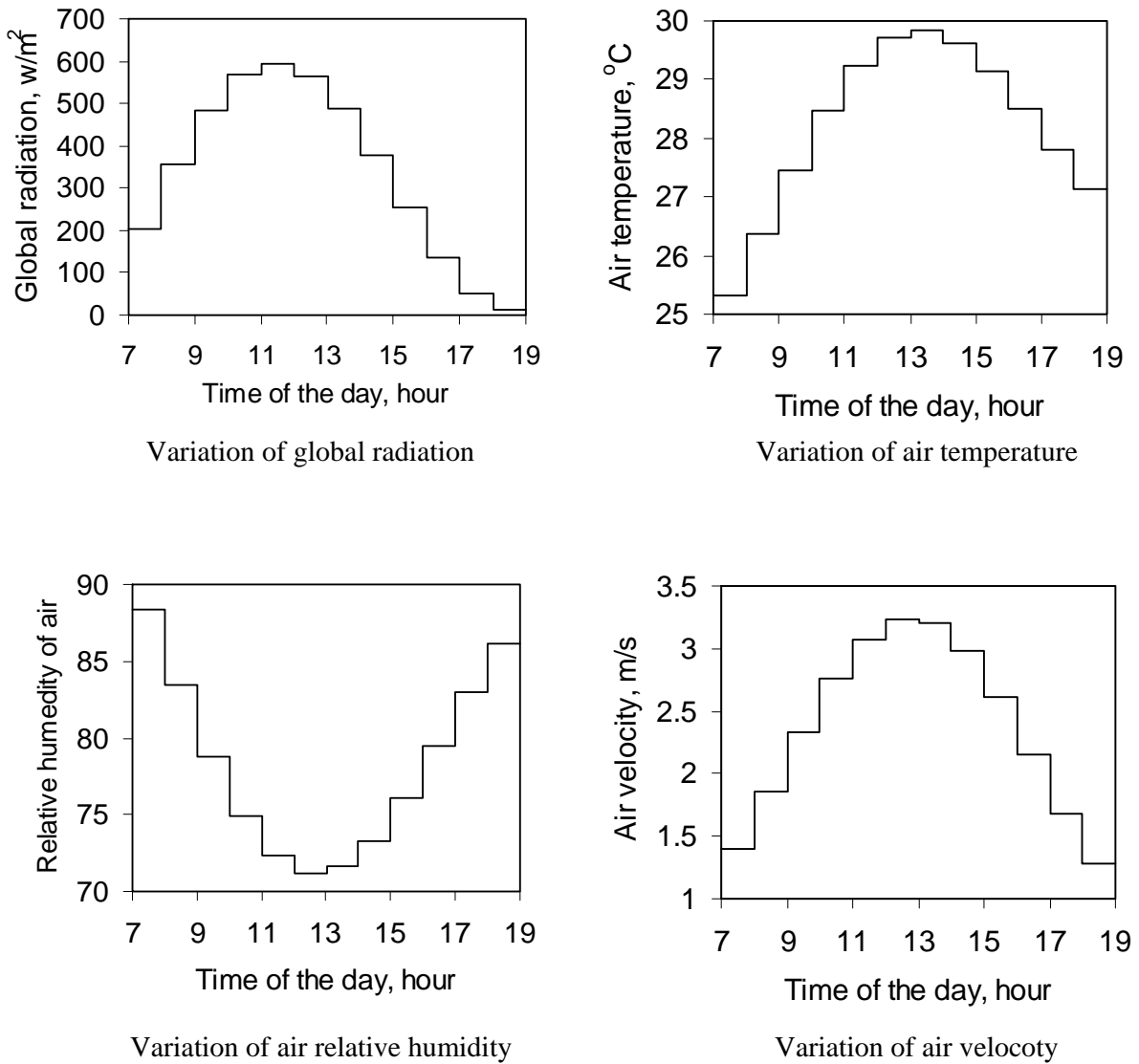


**Figure 32.** Variation of global radiation, air temperature, air relative humidity and air velocity. Locaton: Singapore, Month: October.

- The variation of the flux of moisture with average moisture content of the product for sun drying is shown in Figure 33.
- The variation of average moisture content of the product with drying time for sun drying is shown in Figure 34.

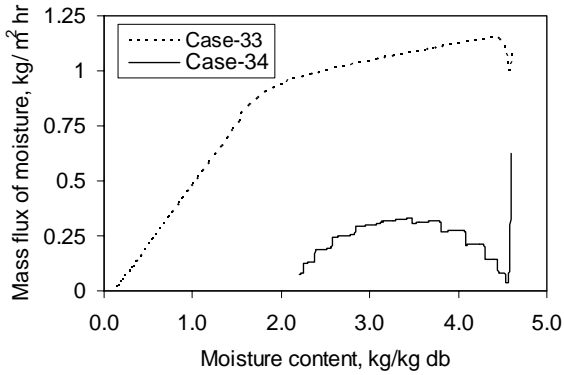


**Figure 33** Variation of moisture flux with average moisture content for sun drying

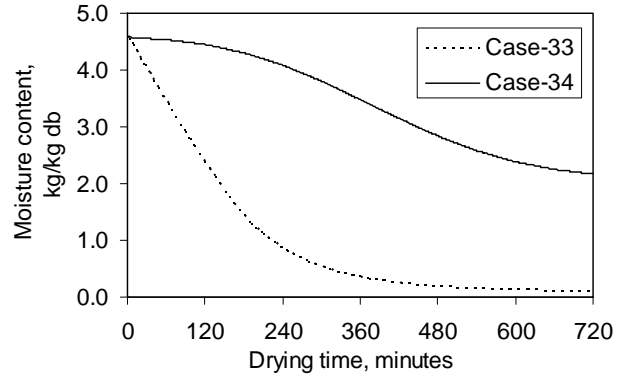


**Figure 34** Variation of average moisture content with drying time for sun drying

## 5. CONCLUSIONS

A simple liquid diffusion model with moisture and temperature dependent effective mass diffusivity and thermal conductivity was used to simulate batch drying of thin shrinking slabs of heat sensitive materials subjected to multiple modes of heat input. Allowance was made for shrinkage and heat of desorption. The relative advantages of combining various modes of heat transfer e.g. convection, conduction, radiation and volumetric heating with microwave field were analyzed using the predicted moisture and temperature distribution, moisture flux and drying rates. On/off type temperature controller was simulated to control the power of the heaters so as not to exceed a pre-specified damage temperature of the material. Microwave heating with convection showed the best overall drying performance. However, a particular combination of heat inputs did not exhibit the “best” drying performance during the whole drying period which reflects the need of appropriate switching between different modes of heat input to get the optimum and energy efficient drying condition. Effects of the stepwise change of drying air temperature, velocity, relative humidity, drying of products of high and low moisture diffusivity, flipping of product, and sun drying on the drying were studied. Simulation results show that drying air temperature and velocity should be high and air relative humidity should be low at the initial period of drying. Flipping of product can improve drying rate significantly especially for thick product. Future work will deal with two dimensional cases with both continuous and time-varying multiple heat inputs and will include the kinetics of quality degradation.

Although very simple mathematically, the diffusion model includes an enormous amount of useful information that can be used in design as well as in optimizing design conditions for best quality or minimum energy expenditure or minimum capital cost. For example, flipping and/or intermittent heating can save air and energy consumption. Using heat pump to dehumidifying air is effective only over a narrow moisture range so one can save on both capital and running costs by using a smaller heat pump only periodically for drying heat sensitive materials like vegetables, fruits, marine foods etc. It can also be used for model based control of the dryer.

## ACKNOWLEDGMENT

The authors acknowledge with gratitude a grant awarded by the National University of Singapore (RP: R-265-000-074-112) under which this work was performed.

## NOMENCLATURE

### *Symbols*

$A$	area of drying surface, $m^2$
$A_w$	water activity
$C_p$	specific heat of product, $J/kg\ K$
$D_{AB}$	water diffusivity in product, $m^2/s$
$D_{vp,air}$	diffusivity of vapor in air, $m^2/s$
$H$	product thickness, $m$
$\Delta H_w$	heat of wetting, $J/kg$
$h_{air}$	convective heat transfer coefficient in air, $W/m^2\ K$
$h_f$	enthalpy of saturated water, $J/kg$
$h_{fg}$	latent heat of vaporization, $J/kg$
$h_g$	enthalpy of saturated vapor, $J/kg$
$h_m$	mass transfer coefficient of vapor in air, $m/s$
$h_{vap}$	heat of vaporization, $J/kg$
$J_{m,s}$	mass flux of water vapor, $kg\ of\ moisture/m^2\ s$
$k$	thermal conductivity, $W/m\ K$
$M_w$	molecular weight of water, $kg/kmol$
$\Delta m_{solid,i}$	mass of bd solid in $i^{th}$ control volume, $kg$
$n$	number of control volume
$Nu$	Nusselt number, $\frac{h_{air}\Delta Y}{k_{air}}$
$P$	total pressure, $Pa$
$P_{air}$	partial pressure of air, $Pa$
$P_v$	partial pressure of vapor, $Pa$
$Pr$	Prandtl number, $\frac{\nu_{air}}{\alpha_{air}}$
$P_{v,sat}$	saturated vapor pressure, $Pa$
$\dot{q}_{conv}$	convection heat flux, $W/m^2$
$\dot{q}_{heater}$	conduction heat flux, $W/m^2$
$\dot{q}_{rad}$	radiation heat flux, $W/m^2$
$\dot{q}_{vapor}$	heat flux with evaporated moisture, $W/m^2$
$Q_{mw}$	microwave source, $W/m^3$
$R$	universal gas constant, $J/(kmol\ K)$
$Re$	Reynolds number, $\frac{\rho_{air}V_{air}\Delta Y}{\mu_{air}}$
$Sc$	Schmidt number, $\frac{\mu_{air}}{\rho_{air}D_{vp,air}}$
$Sh$	Sherwood number, $\frac{h_m}{\Delta Y D_{vp,air}}$
$T$	temperature, $^{\circ}C$
$t$	time, $sec$
$V$	velocity of drying air, $m/s$
$X_m$	moisture content, $kg\ moisture/kg\ db$
$Z$	axis along product thickness, $m$

$\Delta Y$  product length, m

### ***Greek Letters***

$\alpha$  thermal diffusivity, m<sup>2</sup>/s  
 $\mu$  absolute viscosity, kg/(m s)  
 $\nu$  kinematic viscosity, m<sup>2</sup>/s  
 $\rho_p$  density of product, kg/m<sup>3</sup>  
 $\rho_m$  moisture concentration in product, kg of moisture/m<sup>3</sup> product  
 $\rho_w$  density of water, kg/m<sup>3</sup>  
 $\rho_{\text{solid}}$  density of bd solid, kg/m<sup>3</sup>  
 $\phi$  air relative humidity  
 $\beta$  attenuation constant  
 $\varepsilon_p$  absorptivity of product  
 $\varepsilon'$  dielectric constant  
 $\varepsilon''$  dielectric loss factor  
 $\lambda_{\text{mw,v}}$  microwave wavelength in vacuum, m  
 $\sigma$  Stefan and Boltzman constant,  $5.67 \times 10^{-8}$  W/(m<sup>2</sup> K<sup>4</sup>)

### ***Subscripts***

*air* drying air  
*p* product  
*o* initial  
*rad* radiation heater  
*sat* saturation  
*v* vapor

**Table 1** The thermodynamics and transport properties of air and water systems and the physical properties of the potato sample

Property	Reference	Expression
$\rho_{air}$ ( $kg\ m^{-3}$ )	Oosthuizen and Naylor, (1999)	$\rho_{air} = -3.510101x10^{-8}T_{air}^3 + 1.583982684x10^{-5}T_{air}^2 - 4.69952020202x10^{-3}T_{air} + 1.29213571428571;$ ( $10^{\circ}C < T_{air} < 80^{\circ}C$ )
$\mu_{air}$ ( $kg\ m^{-1}\ s^{-1}$ )	Oosthuizen and Naylor, (1999)	$\mu_{air} = 1.7676768x10^{-13}T_{air}^3 - 5.541125541x10^{-11}T_{air}^2 + 4.983297258297x10^{-8}T_{air} + 17.1964285714285x10^{-6};$ ( $10^{\circ}C < T_{air} < 80^{\circ}C$ )
$Pr_{air}$	Oosthuizen and Naylor, (1999)	$Pr_{air} = -2.272727x10^{-8}T_{air}^3 + 4.1991342x10^{-6}T_{air}^2 - 3.5335497835x10^{-4}T_{air} + 0.719;$ ( $10^{\circ}C < T_{air} < 80^{\circ}C$ )
$k_{air}$ ( $W\ m^{-1}\ K^{-1}$ )	Oosthuizen and Naylor, (1999)	$k_{air} = 6.8181818x10^{-10}T_{air}^3 - 1.474025974x10^{-7}T_{air}^2 + 8.029112554113x10^{-5}T_{air} + 0.0240835714285714;$ ( $10^{\circ}C < T_{air} < 80^{\circ}C$ )
$h_{fg}$ ( $kJ\ kg^{-1}$ )	Oosthuizen and Naylor, (1999)	$h_{fg} = -2.394T + 2502.1$
$P_{v,sat}$ ( $Pa$ )	Mujumdar and Devahastin, (2000)	$P_{v,sat} = 100 \exp\left(27.0214 - \frac{6887}{T_p + 273.15} - 5.31 \ln \frac{T_p}{273.16}\right)$
$\rho_p$ ( $kg\ m^{-3}$ )	Senadeera et al., (2000)	$\rho_p = -10^{-3}X_m^4 - 6.4X_m^3 + 55X_m^2 - 154X_m + 1253$
$k_p$ ( $W\ m^{-1}\ K^{-1}$ )	Saravacos and Maroulis, (2001)	$k_p = \frac{0.049}{1 + X_m} \exp\left[-\frac{47}{8.3143x10^{-3}}\left(\frac{1}{T_p + 273.15} - \frac{1}{333.15}\right)\right] + \frac{0.611X_m}{1 + X_m}$
$D_{AB}$ ( $m^2\ s^{-1}$ )	Sablani et al., (2000)	$D_{AB} = 1.29x10^{-6} \exp\left(\frac{-0.0725}{X_m}\right) \exp\left(\frac{-2044}{T_p + 273.15}\right)$
$A_w$	Saravacos and Maroulis, 2001; Rahman, 1995	$A_w = 1232.3X_m^4 - 646.14X_m^3 + 98.541X_m^2 - 0.3406X_m - 0.0008;$ ( $X_m < 0.22$ ) $A_w = -0.51294646815992X_m^2 + 0.63981302510109X_m + 0.59948289559041;$ ( $0.22 \leq X_m \leq 0.6$ ) $A_w = 0.0013X_m^3 - 0.0197X_m^2 + 0.1164X_m + 0.7448;$ ( $X_m > 0.6$ )
$H_w$ ( $kJ\ kg^{-1}$ )	Keey, (1972)	$H_w = 8.206767191142x10^6 X_m^4 + 4.00032779720271x10^6 X_m^3 - 6.1613964160838x10^5 X_m^2 + 2.368187645688x10^4 X_m + 1.16308333333x10^3;$ ( $0.01 \leq X_m \leq 0.2$ )

## REFERENCES

- Chen, G.; Wang, W.; Mujumdar, A.S. Theoretical Study of Microwave Heating Patterns on Batch Fluidized Bed Drying of Porous Material. *Chemical Engineering Science* **2001**, *56*, 6823-6835.
- Chen, P.; Pei, D.C.T. A mathematical Model of Drying Processes. *International Journal of Heat and Mass Transfer* **1989**, *32* (2), 297-310.
- Chen, P.; Schmidt, P.S. An integral Model for Convective Drying of Hygroscopic and Nonhygroscopic Materials. In *Drying '89*; Mujumdar, A.S., Ed.; Hemisphere: Washington, DC, 1989; 162-218.
- Chou, S.K.; Chua, K.J.; Mujumdar, A.S.; Tan, M.; Tan, S.L. Study on the osmotic pre-treatment and infrared radiation on drying kinetics and colour changes during drying of agricultural products. *Asean Journal on Science & Technology for Development* **2001**, *18* (1), 11-23.
- Chou, S.K.; Chua, K.J.; Mujumdar, A.S.; Hawlader, M.N.A.; Ho, J.C. On the Intermittent Drying of an Agricultural Product. *Trans IChemE* **2000**, *78*, 193-203.
- Chou, S.K.; Hawlader, M.N.A.; Ho J.C.; Chua, K. J. The contact factor for dryer performance and design. *International Journal of Energy Research* **1999**, *23*, 1277-1291.
- Chou, S.K.; Hawlader, M.N.A.; Chua, K.J. On the drying of food products in a tunnel dryer. *Drying Technology-An International Journal* **1997**, *15* (3 & 4), 857-880.
- Chua, K.J.; Chou, S.K.; Hawlader, M.N.A.; Mujumdar, A.S.; Ho, J.C. Modelling the moisture and temperature distribution within an agricultural product undergoing time-varying drying schemes. *Biosystems Engineering* **2002**, *81*(1), 99-111.
- Chua, K.J., Mujumdar, A.S., Hawlader, M.N.A., Chou, S.K., and Ho, J.C. Study of stepwise change in drying air temperature during batch drying of agricultural products. *Food Research International* **2001**, *34*, 721-731.
- Chua, K.J.; Chou, S.K.; Ho, J.C.; Mujumdar, A.S.; Hawlader, M.N.A. Cyclic air temperature drying of guava pieces: Effects on moisture and ascorbic acid contents. *Transactions of the Institution of Chemical Engineers* **2000**, *78*, Part C, 72-78.
- Chua, K.J.; Mujumdar, A.S.; Chou, S.K.; Hawlader, M.N.A.; Ho, J.C. Convective drying of banana, guava and potato pieces: Effect of cyclical variations of air temperature on convective drying kinetics and colour change. *Drying Technology-An International Journal* **2000**, *18* (5), 907-936.
- Chua, K.J. Dynamic Modeling, *Experimentation and Optimisation of Heat Pump Drying for Agricultural Products*, Ph.D Thesis, National University of Singapore, Singapore-119260; 2000; 1-1 – 10-11.
- Coumans, W.J. Models of Drying Kinetics Based on Drying Curves of Slabs. *Chemical Engineering and Processing* **2000**, *39*, 53-68.
- Elbert, G.; Tolaba, M.P.; Aguerre, R.J.; Suarez, C. A diffusional Model with a Moisture Dependent Diffusion Coefficient for Parboiled Rice. *Drying Technology – An International Journal* **2001**, *19* (1), 155-166.

Etter, D.M. *Engineering problem solving with Matlab*; Prentice hall, Englewood cliffs, New Jersey 07632, 1993.

Hawlder, M.N.A.; Ho, J.C.; Qing, Z. A Mathematical Model for Drying of Shrinking Materials. *Drying Technology – An International Journal* **1999**, *17* (1 & 2), 27-47.

Hawlder, M.N.A.; Bong T.Y.; Mahmood, Wang. Some Frequently Used Meteorological Data For Singapore. *Internal Journal of Solar Energy* **1990**, *8*, 1-11.

Herman, E.; Rodriguez, G.C.; Garcia, M.A. Mathematical Modeling for Fixed-Bed Drying Considering Heat and Mass Transfer and Interfacial Phenomena. *Drying Technology – An International Journal* **2001**, *19* (9), 2343-2362.

Ho, J.C.; Chou, S.K.; Chua, K.J.; Mujumdar, A.S.; Hawlder, M.N.A. Analytical Study of Cyclic Temperature Drying: Effect of Drying Kinetics and Product Quality. *Journal of Food Engineering* **2002**, *51*, 65-75.

Ho, J.C.; Chou, S.K.; Mujumdar, A.S.; Hawlder, M.N.A.; Chua, K.J. An optimisation framework for drying of a heat-sensitive product. *Applied Thermal Engineering* **2001**, *21*, 1779-1798.

Hosseinalipour, S.M.; Mujumdar A.S. A Model for Superheated Steam Drying of Particles in an Impinging Steam Dryer. In *Mathematical Modeling and Numerical Techniques in Drying Technology*; Turner, I., Mujumdar, A.S., Eds.; Marcel Dekker, Inc.: New York, 1997; 537-574.

Kardum, J.P.; Sander, A.; Skansi, D. Comparison of Convective, Vacuum and Microwave Drying Chlorpropamide. *Drying Technology – An International Journal* **2001**, *19* (1), 167-183.

Key, R.B. *Drying Principles and Practice*, 1st Ed.; Pergamon Press: Oxford, New York, 1972.

Key, R.B. *Introduction to Industrial Drying Operations*, Pergamon Press: Oxford, New York, 1978.

Liu, J.Y.; Simpson W.T. Two-Stage Moisture Diffusion in Wood with Constant Transport Coefficients. *Drying Technology – An International Journal* **1999**, *17* (1&2), 257-269.

Madhiyanon, T.; Soponronnarit, S.; Tia, W. A Mathematical Model for Continuous Drying of Grains in a Spouted Bed Dryer. *Drying Technology – An International Journal* **2002**, *20* (3), 587-614.

Mujumdar, A.S. Drying Technologies of the Future. *Drying Technology - An International Journal* **1991**, *9* (2), 325-347.

Mujumdar, A.S.; Devahastin, S. *Drying: Thermodynamics and Fundamentals, Developments in Drying, Food Dehydration*; Kasetsart University Press: Bangkok, Thailand, 2000; vol. 1, 5-42.

Mujumdar, A.S.; Devahastin, S. *Fundamental Principles of Drying, Mujumdar's Practical Guide to Industrial Drying*, Exergex Corporation: 3795 Navarre, Brossard, Quebec, Canada, 2000.

Mujumdar, A.S. *Handbook of Industrial Drying*, Chapter 1 & 2, 2nd Ed.; Marcel Dekker Inc.: New York, 1995.

Oosthuizen, P.H.; Naylor, D. *An introduction to Convective Heat Transfer Analysis*, WCB/McGraw Hill: New York, 1999.

Pordage, L.J.; Langrish T.A.G. Simulation of the Effect of Air Velocity in the Drying of Hardwood Timber. *Drying Technology – An International Journal* **1999**, *17* (1&2), 237-255.

Raderer, M. *Drying of Viscous, Shrinking Products: Modeling and Experimental Validation*, Ph.D. Thesis, Technical University of Munich, Germany 2001; 1-121.

Rahman, S. *Food Properties Handbook*, CRC Press, Inc.: New York, 1995.

Ranjan, R.; Irudayaraj, J.; Jun, S. Simulation of Infrared Drying Process. *Drying Technology – An International Journal* **2002**, *20* (2), 363-379.

Sablani, S.; Rahman, S.; Al-Habsi, N. Moisture Diffusivity in Foods – An Overview. In *Drying Technology in Agriculture and Food Sciences*; Mujumdar, A.S., Ed.; Science Publishers, Inc.: USA, 2000, 35-59.

Sanga, E.C.M.; Mujumdar, A.S.; Raghavan, G.S.V. Simulation of Convection-Microwave Drying for a Shrinking Material. *Chemical Engineering and Processing* **2002**, *41*, 487-499.

Saravacos, G.D.; Maroulis, Z.B. *Transport Properties of Foods*; Marcel dekker, Inc.: New York, 2001.

Senadeera, W.; Bhandari, B.; Young, G.; Wijesinghe, B. Physical Property Changes of Fruits and Vegetables During Hot Air Drying. In *Drying Technology in Agriculture and Food Sciences*; Mujumdar, A.S., Ed.; Science Publishers, Inc.: USA, 2000, 149-166.

Vinjamur, M.; Cairncross, R.A. A High Airflow Drying Experimental Set-Up to Study Drying Behavior of Polymer Solvent Coatings. *Drying Technology – An International Journal* **2001**, *19* (8), 1591-1621.